J. Fluid Mech. (1992), *vol.* 244, *pp.* 79–100

Three-dimensional nonlinear blow-up from a nearly planar initial disturbance, in boundary-layer transition: theory and experimental comparisons

By P. A. STEWART† AND F. T. SMITH
Department of Mathematics, University College London, Gower Street, London WC1E 6BT, UK

(Received 5 February 1992 and in revised form 25 April 1992)

This theoretical study describes how three-dimensional nonlinear distortion may soon take effect, following a small initial input disturbance that is nearly planar, in an otherwise two-dimensional boundary layer at high Reynolds number. The mechanism involved is a form of vortex–wave interaction, the first such to be examined in the so-called high-frequency range. The interaction is powerful, in that three-dimensional disturbances of relatively low amplitude (the wave part) interact nonlinearly with the three-dimensional corrections to the mean flow (the vortex part) at a stage where the purely two-dimensional case alone would still be linear. A coupled nonlinear partial-differential system is derived, governing the vortex and wave parts. Computations and analysis of the system are then presented. These point to a finite-time singularity arising in the solution, involving blow-up of both the vortex and the wave amplitudes (but particularly the former), accompanied by spanwise focusing into streets. This is believed to be the first nonlinear interaction in the high-frequency range to produce a finite-time (or-distance) blow-up. The blow-up is such that the local flow soon enters a strongly nonlinear three-dimensional stage in which the total mean flow is altered. The implications of this blow-up and focusing for one of the classic paths of boundary-layer transition are also discussed, and here quantitative and/or order-of-magnitude comparisons suggest that the theory is in line with the findings of Klebanoff & Tidstrom (1959) and later experiments.

1. Introduction

One of the classic types of boundary-layer transition to turbulence seen and measured experimentally (in studies stretching from Schubauer & Skramstad 1947; Klebanoff & Tidstrom 1959; and references in Stuart 1963 (e.g. see his figures IX.26–IX.28) to the works referenced in Kleiser & Zang 1991; Hall & Smith 1991) consists of the downstream progression from initially near-planar linear Tollmien–Schlichting (TS) disturbances to three-dimensional nonlinear disturbances and onward to full turbulence, possibly via the production of turbulent spots. This forms perhaps the most well-known path through transition, and it has also been simulated numerically in a number of computations (e.g. see references in Kleiser & Zang 1991). It provides the motivation for the present theoretical study. Here our attention is on nonlinear interactions between TS waves and their induced vortex motion, interactions which are three-dimensional of necessity and can take place at

† Current address: School of Mathematics, The University, Leeds, LS2 9JT, UK.

surprisingly low wave amplitudes as we see below. The particular type of transition that arises in practice, as well as in theory, depends on the amplitudes, wavenumbers and frequencies of the input disturbance upstream, and on the general disturbance environment, and there are indeed many types and paths, including the by-pass type. The specific concern here is in inputs that are relatively small and almost two-dimensional initially. The main applications in mind are to aerodynamic and to atmospheric boundary layers although there are a number of other related applications.

Of special interest on the theoretical side is the so-called high-frequency range (Smith & Burggraf 1985; Smith & Stewart 1987; Stewart & Smith 1987), based on the triple-deck account of how nonlinearity can first affect two- or three-dimensional TS disturbances near the lower branch of the neutral curve (Smith 1979*a*, *b*). This range extends in fact towards the upper branch (see references above, and the extensions in Smith, Doorly & Rothmayer 1990) and it is a very interesting range experimentally as well as theoretically. For instance, Smith & Stewart (1987), following Craik (1971), show that the high-frequency range provides an explanation of the resonant-triad nonlinear interaction, including very good agreement with the experiments of Kachanov & Levchenko (1984). Again, there is good agreement between the theory of Stewart & Smith (1987) and the experiments of Kachanov (1988) concerning the instability of separating flow, while the recent paper by Kachanov, Ryzhov & Smith (1992) indicates very close alignment of the nonlinear two-dimensional theory (see Smith & Burggraf 1985; Zhuk & Ryzhov 1982) and the experiments of Kachanov and co-workers (Borodulin & Kachanov 1988; Kachanov 1988). Our interest however is in the case of nearly two-dimensional input, and how it may succumb nonlinearly to three-dimensional distortion, as distinct from both the strictly two-dimensional input of Smith & Burggraf (1985) and the rather specific three-dimensional input of Smith & Stewart (1987), Craik (1971). In particular, we are concerned with the effects of vortex–wave interaction (VWI) in the high-frequency range, for an otherwise two-dimensional incompressible boundary layer.

The VWI considered below starts its life as a weakly nonlinear interaction as described later. The wave part of the VWI has amplitudes that are much less than those in the alternative, purely planar, development (Smith & Burggraf 1985; Smith 1985, 1986*a*) but happen to be comparable with those in the resonant-triad interaction of Smith & Stewart (1987), which forms another alternative path. In the current work, a substantial part of which was done during the period 1987–89, it is the response of the vortex part or mean-flow correction of the VWI that is crucial, as found in other work (e.g. Hall & Smith 1988, 1989, 1990, 1991; Smith & Walton 1989; Bassom & Hall 1990; Smith & Blennerhassett 1992; Walton & Smith 1992; Smith 1992). The vortex velocity induced in the streamwise direction is notably large due to the inertial action of wave-amplitude-squared effects on the relatively small spanwise momentum of the vortex, combined with the relatively slow temporal–spatial evolution of the vortex flow; see §2 below. The second harmonics, in contrast, play no significant part in the VWI and neither does the induced critical layer in this regime as the critical layer is nonlinear and passive. It is interesting that the current VWI appears to be the first one studied in the high-frequency range. In fact, it connects the three strongly nonlinear transition theories listed by Hall & Smith (1991), namely pressure–displacement interaction theory (Smith 1979*a*, *b*, 1988; Peridier, Smith & Walker 1991*a*, *b*; Hoyle, Smith & Walker 1991; Smith & Bowles 1992), Euler-scale theory (Smith & Burggraf 1985; Smith *et al.* 1990), and vortex–wave interaction theory (see references earlier in this paragraph). In any

case, the VWI here is controlled by a nonlinear coupled partial-differential system linking the temporal-spatial development of the vortex and wave parts, as §2 shows. Computational and analytical properties are presented in §§3, 4, the most significant property being that the VWI solution develops a singularity within a finite scaled time. Further comments and repercussions, together with quantitative comparisons between the theory and experiments, are given in §5.1–5.3.

This is the first weakly nonlinear interaction found (in the high-frequency range) to provoke a blow-up within a finite time, as far as we can tell. In that sense, it represents the most powerful nonlinear effect found, so far anyway. Moreover, the blow-up occurs before purely two-dimensional nonlinearity would have come into the reckoning (see also further comments in §5.1).

An equally significant feature is that the nature of the blow-up implies that a strongly nonlinear stage is soon encountered next (see §5.2), accompanied by spanwise focusing into streets; this feature among others is found to agree with the experimental findings of Klebanoff & Tidstrom (1959) as summarized in Stuart's (1963) figures IX.26–IX.28 (see §5.3) and later experiments (e.g. Klebanoff, Tidstrom & Sargent 1962, Kovasznay, Komoda & Vasudeva 1962; Hama & Nutant 1963; Nishioka, Asai & Iida 1979). Thus the present VWI provides a means for small almost two-dimensional input to reach large three-dimensional status relatively fast and alter the total mean flow. This is described in detail in §5.2, along with several other issues that arise (§5.1), followed by the comparisons in §5.3.

The present setting, then, starts with the incompressible triple-deck scales (see also below), in which

$$[u_{\rm D}, v_{\rm D}, w_{\rm D}]/u_{\rm D\infty} = [Re^{-\frac{1}{8}}u, Re^{-\frac{3}{8}}v, Re^{-\frac{1}{8}}w], \quad (p_{\rm D}-p_{\rm D\infty})/\rho_{\rm D}\,u_{\rm D\infty}^2 = Re^{-\frac{1}{4}}p, \quad (1.1a, b)$$

$$[x_{\rm D}-x_{\rm D0}, y_{\rm D}, z_{\rm D}-z_{\rm D0}]/l_{\rm D} = [Re^{-\frac{3}{8}}x, Re^{-\frac{5}{8}}y, Re^{-\frac{3}{8}}z], t_{\rm D}\,u_{\rm D\infty}/l_{\rm D} = Re^{-\frac{1}{4}}t \quad (1.1c, d)$$

in the lower deck. Here (1.1*a*) gives the velocity vector in the Cartesian coordinates of (1.1*c*) (streamwise, normal, spanwise respectively), $p_{\rm D}$ is the pressure, and $t_{\rm D}$ is the time, while the subscript D denotes dimensional variables and ∞ denotes local free-stream values, near the position $(x_{\rm D0}, z_{\rm D0})$ of concern. The fluid density $\rho_{\rm D}$ and the lengthscale $l_{\rm D}$ (e.g. the airfoil chord) are constants and the Reynolds number $Re \equiv u_{\rm D\infty}\,l_{\rm D}/\nu_{\rm D}$ is large, with $\nu_{\rm D}$ being the kinematic viscosity of the fluid. The usual skin-friction factor λ is normalized to unity, without loss of generality, and the wall is given by $y = 0$. Under (1.1*a–d*), the Navier–Stokes equations reduce to the unsteady nonlinear interactive boundary-layer equations (2.1*a–c*) below, subject to boundary conditions (in (2.1*d–f*)) which, among other things, match the solutions in the three decks of the triple-deck structure. The system (2.1*a–f*) supports linear and nonlinear two- and three-dimensional TS waves and VWI's, apart from the high-frequency range, and the system also produces predictions in good agreement with experiments or direct numerical simulations in certain cases. Hence we start with that system, although in fact the high-frequency range adopted subsequently applies for a wide range of scales beyond those given in (1.1*a–d*), as earlier papers have noted. The current VWI raises some interesting questions about the interplay with other interactions such as resonant triads, and it may yield insight into new VWI structures near the linear upper branch, e.g. concerning the crossover from TS to Rayleigh-like nonlinear interactions.

2. Flow structure, and derivation of the VWI

Given the arguments presented in §1, we work in terms of the three-dimensional triple-deck problem, requiring a solution of the unsteady nonlinear three-dimensional interactive boundary-layer equations

$$\frac{\partial u}{\partial x}+\frac{\partial v}{\partial y}+\frac{\partial w}{\partial z}=0, \tag{2.1a}$$

$$\frac{\partial u}{\partial t}+u\frac{\partial u}{\partial x}+v\frac{\partial u}{\partial y}+w\frac{\partial u}{\partial z}=-\frac{\partial p}{\partial x}+\frac{\partial^2 u}{\partial y^2}, \tag{2.1b}$$

$$\frac{\partial w}{\partial t}+u\frac{\partial w}{\partial x}+v\frac{\partial w}{\partial y}+w\frac{\partial w}{\partial z}=-\frac{\partial p}{\partial z}+\frac{\partial^2 w}{\partial y^2}, \tag{2.1c}$$

with $\partial p/\partial y$ zero and the pressure $p(x,z,t)$ being unknown. These are subject to the main boundary conditions

$$u=v=w=0 \quad \text{at} \quad y=0, \tag{2.1d}$$

$$u\sim y+A(x,z,t), \quad w\to 0 \quad \text{as} \quad y\to\infty, \tag{2.1e}$$

$$p(x,z,t)=-\frac{1}{2\pi}\int_{-\infty}^{\infty}\int_{-\infty}^{\infty}\frac{\partial^2 A}{\partial\xi^2}(\xi,\eta,t)\frac{\partial\xi\,\partial\eta}{[(x-\xi)^2+(z-\eta)^2]^{\frac{1}{2}}}, \tag{2.1f}$$

from the no-slip condition at the fixed surface, from the matching involving the unknown displacement function $-A$, and from the interaction with the external flow, respectively. This last condition can also be expressed in the form of solving Laplace's equation for the pressure just outside the boundary layer,

$$(\partial_x^2+\partial_{\bar y}^2+\partial_z^2)\bar p=0, \tag{2.1g}$$

with

$$\bar p\to p, \quad \frac{\partial\bar p}{\partial\bar y}\to\frac{\partial^2 A}{\partial x^2} \quad \text{as} \quad \bar y\to 0, \tag{2.1h}$$

and with suitably bounded far-field conditions, as an alternative to (2.1*f*).

Our concern then is with the range of relatively high frequencies, or fast travelling nonlinear disturbances, similar to that in Smith & Burggraf (1958), Smith (1985, 1986*a*, *b*), Smith & Stewart (1987), Stewart & Smith (1987). Thus now

$$\frac{\partial}{\partial t}\to\frac{\Omega\partial}{\partial T_0}+\frac{\partial}{\partial T_2}+\ldots, \quad \frac{\partial}{\partial x}\to\Omega^{\frac{1}{2}}\frac{\partial}{\partial X_0}+\Omega^{-\frac{1}{2}}\frac{\partial}{\partial X_2}+\ldots, \quad \frac{\partial}{\partial z}\to\frac{\partial}{\partial Z_1}+\Omega^{-1}\frac{\partial}{\partial Z_3}+\ldots, \tag{2.2a–c}$$

with the effective frequency parameter Ω being large. Here $t=\Omega^{-1}T_0=T_2=\ldots$, $x=\Omega^{-\frac{1}{2}}X_0=\Omega^{\frac{1}{2}}X_2=\ldots$, $z=Z_1=\ldots$ define the multiple variables present, and the main difference from the works mentioned just above is the particular form of the multiple-scales dependence in (2.2*a–c*), especially the relatively slow spanwise variation, and the three-dimensional expansions set out below. The pressure and displacement fields for the current context of VWI's are given by the expansions

$$p=(P_0E+P_0^*E^{-1})+\Omega^{-1}P_2+O(\Omega^{-\frac{3}{2}}), \tag{2.3a}$$

$$A=\Omega^{-\frac{1}{2}}(A_0E+A_0^*E^{-1}+A_{0M})+\Omega^{-\frac{3}{2}}A_2+\ldots \tag{2.3b}$$

(* or c.c. denotes the complex conjugate) where the dominant wave-like dependence is two-dimensional, such that

$$E\equiv\exp[\mathrm{i}(\alpha_0X_0-T_0)], \tag{2.4}$$

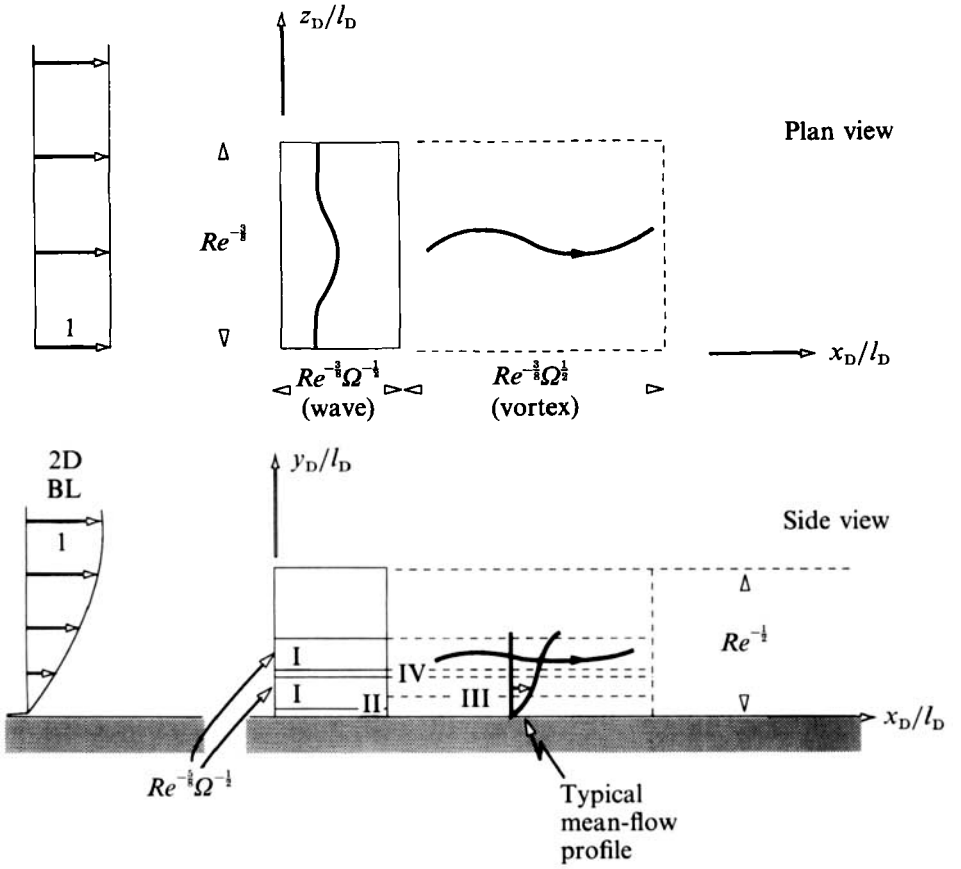

FIGURE 1. Sketch of the VWI flow structure for near-planar input, showing the lower-deck regions I–IV and the main part of the $O(Re^{-\frac{1}{2}})$ boundary layer, within the high-frequency range, in non-dimensional terms. The diagram is not to scale, and the outer potential-flow zone or upper deck is not shown. This structure should be compared with that in figure 5 below.

while the velocity field subdivides into four distinct regions (I–IV) in the normal direction, as described below; see also figure 1. In (2.3*a*, *b*), $(P_0, A_0, A_{0M})\,(X_2, Z_1, T_2)$ are unknown, as are P_2, A_2 which are given in more detail subsequently.

The major region (I) is an inviscid one in which y is large, $y = \Omega^{\frac{1}{4}}\hat{y}$ with $\hat{y}$ typically of order unity, and the velocity components expand in the form

$$u = \Omega^{\frac{1}{4}}\hat{y} + \Omega^{-\frac{1}{4}}U_0 + \Omega^{-\frac{3}{4}}U_2 + \ldots, \quad v = \Omega^{\frac{1}{4}}V_0 + \Omega^{-\frac{1}{4}}V_2 + \ldots, \quad w = \Omega^{-1}W_1 + \Omega^{-2}W_3 + \ldots, \tag{2.5a–c}$$

where we observe the relative weakness of the spanwise velocity. Substitution of (2.5*a–c*), along with (2.3*a*), into the controlling equations (2.1*a–c*) therefore yields in turn the following sets of successive equations:

for continuity
$$\frac{\partial U_0}{\partial X_0} + \frac{\partial V_0}{\partial \hat{y}} = 0, \quad \frac{\partial U_0}{\partial X_2} + \frac{\partial U_2}{\partial X_0} + \frac{\partial V_2}{\partial \hat{y}} + \frac{\partial W_1}{\partial Z_1} = 0; \tag{2.6a, b}$$

for x-momentum
$$\frac{\partial U_0}{\partial T_0} + \hat{y}\frac{\partial U_0}{\partial X_0} + V_0 = -(\mathrm{i}\alpha_0 E P_0 + \text{c.c.}), \tag{2.7a}$$

$$\frac{\partial U_0}{\partial T_2} + \frac{\partial U_2}{\partial T_0} + \hat{y}\left(\frac{\partial U_0}{\partial X_2} + \frac{\partial U_2}{\partial X_0}\right) + U_0\frac{\partial U_0}{\partial X_0} + V_2 + V_0\frac{\partial U_0}{\partial \hat{y}} = -\left(E\frac{\partial P_0}{\partial X_2} + \text{c.c.}\right) - \frac{\partial P_2}{\partial X_0}; \tag{2.7b}$$

for z-momentum

$$\frac{\partial W_1}{\partial T_0}+\hat{y}\frac{\partial W_1}{\partial X_0}=-\left(E\frac{\partial P_0}{\partial Z_1}+\text{c.c.}\right), \tag{2.8a}$$

$$\frac{\partial W_1}{\partial T_2}+\frac{\partial W_3}{\partial T_0}+\hat{y}\left(\frac{\partial W_1}{\partial X_2}+\frac{\partial W_3}{\partial X_0}\right)+U_0\frac{\partial W_1}{\partial X_0}+V_0\frac{\partial W_1}{\partial \hat{y}}=-\left(E\frac{\partial P_0}{\partial Z_3}+\text{c.c.}\right)-\frac{\partial P_2}{\partial Z_1}, \tag{2.8b}$$

in turn.

The solutions relevant here have the form

$$U_0=EU_{01}+\text{c.c.}+U_{0\text{M}},\quad U_2=E^2U_{22}+EU_{21}+\text{c.c.}+U_{2\text{M}}, \tag{2.9a, b}$$

$$W_1=EW_{11}+\text{c.c.}+W_{1\text{M}}, \tag{2.9c}$$

with any E-dependence being shown explicitly, and likewise for the v-components except that $V_{0\text{M}}$ is zero. In (2.9) it is noteworthy that the mean-flow correction terms, i.e. the mean vortex components, are comparable with the fundamentals, in both the streamwise and the spanwise velocities. From (2.6a) ff. and from the constraints in (2.1d–f) (see also Appendix A), we obtain

$$U_{01}=\alpha_0 P_0,\quad V_{01}=-\mathrm{i}\alpha_0^2\hat{y}P_0,\quad A_0=P_0,\quad \alpha_0=1, \tag{2.10a–d}$$

$$W_{11}=\mathrm{i}(\hat{y}-1)^{-1}\partial P_0/\partial Z_1, \tag{2.10e}$$

for the main fundamentals ($\propto E$), while from the higher-order balances the mean-flow corrections ($\propto E^0$) are governed by

$$\frac{\partial U_{0\text{M}}}{\partial X_2}+\frac{\partial V_{2\text{M}}}{\partial \hat{y}}+\frac{\partial W_{1\text{M}}}{\partial Z_1}=0,\quad \frac{\partial U_{0\text{M}}}{\partial T_2}+\frac{\hat{y}\partial U_{0\text{M}}}{\partial X_2}+V_{2\text{M}}=0, \tag{2.11a, b}$$

$$\frac{\partial W_{1\text{M}}}{\partial T_2}+\frac{\hat{y}\partial W_{1\text{M}}}{\partial X_2}+(\hat{y}-1)^{-2}\frac{\partial(|P_0|^2)}{\partial Z_1}=-\frac{\partial P_{2\text{M}}}{\partial Z_1}, \tag{2.11c}$$

from (2.6b), (2.7b), (2.8b), and the induced extra fundamentals of interest here satisfy

$$\frac{\partial U_{01}}{\partial X_2}+\mathrm{i}\alpha_0 U_{21}+\frac{\partial V_{21}}{\partial \hat{y}}+\frac{\partial W_{11}}{\partial Z_1}=0, \tag{2.12a}$$

$$\frac{\partial U_{01}}{\partial T_2}-\mathrm{i}U_{21}+\hat{y}\left(\frac{\partial U_{01}}{\partial X_2}+\mathrm{i}\alpha_0 U_{21}\right)+\mathrm{i}\alpha_0 U_{0\text{M}}U_{01}+V_{21}+V_{01}\frac{\partial U_{0\text{M}}}{\partial \hat{y}}=-\frac{\partial P_0}{\partial X_2}-\mathrm{i}\alpha_0 P_{21}, \tag{2.12b}$$

from (2.6b), (2.7b), whereas the fundamental's contributions in (2.8b) serve only to control W_{31}. A key term in the mean-flow balances is the last one on the left-hand side of (2.11c), which stems from the nonlinear forcing contributions in (2.8b), with the solutions (2.10a–e) inserted. This term, due to the spanwise variation of the wave amplitude, drives the mean-w field $W_{1\text{M}}$ in (2.11c) which then forces the mean-flow contributions $U_{0\text{M}}$, $V_{2\text{M}}$ via the continuity and streamwise-momentum balances (2.11a, b). Likewise, the mean-flow corrections then act to drive the extra fundamental response in (2.12a, b), along with the relatively slow spanwise dependence and the relatively small viscous effects, as we see below. The second-harmonic contributions play no significant role.

Solving (2.11*a–c*) first, then, for example by taking the normal derivative of (2.11*b*) and applying (2.11*a*, *c*) to give

$$\left(\frac{\partial}{\partial T_2}+\hat{y}\frac{\partial}{\partial X_2}\right)^2\frac{\partial U_{0M}}{\partial \hat{y}} = -\frac{1}{(\hat{y}-1)^2}\frac{\partial^2}{\partial Z_1^2}(|P_0|^2), \tag{2.13a}$$

we find the expression

$$\frac{\partial U_{0M}}{\partial \hat{y}} = -\frac{1}{(\hat{y}-1)^2}\frac{\partial^2}{\partial Z_1^2}\int_{-\infty}^{T_2}(T_2-T_2')|P_0|^2\,(X_2-\hat{y}(T_2-T_2'),Z_1,T_2')\,\mathrm{d}T_2' \tag{2.13b}$$

for the mean shear correction. Here the nonlinear disturbances are supposed to die out at large negative times T_2 (this can be altered readily, e.g. to T_2 starting at zero), while the induced mean pressure term $\partial P_{2M}/\partial Z_1$ in (2.11*c*) is anticipated to be zero due to the lack of a corresponding displacement forcing, which is justified in Appendix A. Second, (2.12*a*, *b*) yield the extra fundamental shear solution

$$\frac{\partial U_{21}}{\partial \hat{y}} = \frac{\hat{y}P_0}{(\hat{y}-1)}\frac{\partial^2 U_{0M}}{\partial \hat{y}^2}+\frac{1}{(\hat{y}-1)^2}\frac{\partial^2 P_0}{\partial Z_1^2} \tag{2.14a}$$

and the integral of this, inserted into (2.12*b*) with $\hat{y}\to 0+$, gives the relation

$$\frac{\partial P_0}{\partial T_2}+\mathrm{i}P_0\left\{\int_0^\infty \frac{1}{(\hat{y}-1)^2}\frac{\partial U_{0M}}{\partial \hat{y}}\,\mathrm{d}\hat{y}+U_{0M}^{(w)}\right\}+V_{21}^{(w)} = \mathrm{i}\left\{\frac{\partial^2 P_0}{\partial Z_1^2}+A_{21}\right\}-\frac{\partial P_0}{\partial X_2}-\mathrm{i}P_{21}, \tag{2.14b}$$

where the superscript (w) refers to evaluation at $\hat{y}=0+$.

There are three other regions in the y-direction (figure 1), a viscous wall layer (II), a buffer zone (III) for the mean flow, and a critical layer (IV). Of these, only the wall layer contributes to closing the system of governing equations for the VWI; cf. other works where the buffer zone is more active. The wall layer II is a Stokes layer effectively, with $y=\Omega^{-\frac{1}{2}}\tilde{y}$, and $\tilde{y}$ is $O(1)$ for an unsteady–viscous force balance; therein $u=O(\Omega^{-\frac{1}{2}})$ from (2.5*a*), (2.10*a*) and $v\equiv O(\Omega^{-\frac{1}{2}})$ by continuity. The latter velocity then provides a viscous displacement or efflux, as far as the major region I is concerned, giving the value

$$V_{21}^{(w)} = 2^{-\frac{1}{2}}(\mathrm{i}-1)P_0, \tag{2.15a}$$

on matching at large $\tilde{y}$, as in Smith & Burggraf (1985), Smith & Stewart (1987) for instance. The buffer zone III in contrast is fixed by the unsteady–viscous balance for the mean-flow corrections, requiring $y=O(1)$ due to the slower timescale and leading to a diffusion equation governing the mean flow there (cf. §5.2). This structure combining II, III near the wall is consistent with the constraint that

$$U_{0M}^{(w)} = 0, \tag{2.15b}$$

as might be expected from (2.11*b*). The fourth region, the critical layer IV near $\hat{y}=1$, is predominantly nonlinear and acts to smooth out the singularities appearing in the solutions for the major region I, e.g. in (2.13), (2.14*a*).

The VWI system is completed by appeal to the pressure–displacement interaction laws inferred from (2.1*f*) or (2.1*g*, *h*), as in Appendix A. These yield the law

$$A_{21} = P_{21}+\mathscr{L} \quad \text{where} \quad \mathscr{L}\equiv \mathrm{i}\frac{\partial P_0}{\partial X_2}-\frac{1}{2}\frac{\partial^2 P_0}{\partial Z_1^2}, \tag{2.15c}$$

in particular. So, with $A_{21}-P_{21}$ replaced by $\mathscr{L}$, and on use of (2.15*a*, *b*), the relation (2.14*b*) can be coupled with (2.13*b*) to provide the two governing equations for the three-dimensional wave pressure P_0 and the mean (vortex) shear correction $\partial U_{0M}/\partial \hat{y}$ in the current VWI.

3. Governing equations, and computational properties

In normalized form, the VWI is found to be governed by the coupled nonlinear equations

$$\frac{\partial P}{\partial T} - \mathrm{i}\frac{\partial^2 P}{\partial Z^2} = P - \mathrm{i}PQ, \qquad \frac{\partial^2 Q}{\partial T^2} = \frac{\partial^2}{\partial Z^2}(|P|^2), \tag{3.1a, b}$$

for $(P, Q)(Z, T)$. Here as our main example we are taking now the case of dependence on $(a_2 T_2 + b_2 X_2)(\equiv \xi)$, rather than on T_2, X_2 individually, with a_2, b_2 being constants, and the normalization involved has

$$P_0 = \tfrac{1}{2}(a_2 + 2b_2)^{-1} a^{-\frac{1}{4}} \exp(-2^{-\frac{1}{4}}\mathrm{i}T_2) P, \quad Z_1 = 2^{-\frac{1}{4}} Z, \tag{3.2a}$$

$$\int_0^\infty (\hat{y} - 1)^{-2} \frac{\partial U_{0M}}{\partial \hat{y}} \, \mathrm{d}\hat{y} = 2^{-\frac{1}{4}} Q, \quad \xi = 2^{\frac{1}{4}}(a_2 + 2b_2) T \tag{3.2b}$$

from (2.13a, b), (2.14b), (2.15a–c). The constant a is given by

$$3a_2^2 a = 1 + (b-1)(b+1)^{-2} + 6b(b-1)(b+1)^{-4} + 12b^2(b+1)^{-5} \ln|b|,$$

where $b = b_2^{-1} a_2$, and it is assumed that $b \neq -1$, $a_2 \neq 0$, $a > 0$, $(a_2 + 2b_2) > 0$; see also §5. The coupling term $\propto PQ$ in (3.1a) represents the effect of the vortex flow (i.e. the mean-flow correction here) on the nonlinear wave development $\propto P$, while in (3.1b) the spanwise variation of the wave amplitude (on the right) acts to control the vortex flow ($\propto Q$). Thus both P, Q are unknowns.

In general a computational solution of (3.1a, b) is necessary; see also Appendix B concerning secondary instability properties. Computations were performed using a spectral method with periodic boundary conditions imposed at $Z = \pm 0.5$, to fix matters. Two sets of initial conditions at $T = 0$ were studied, namely,

$$P = 0.1 + \hat{\pi}_1 \cos(2\pi Z), \quad Q = \frac{\partial Q}{\partial T} = 0 \quad \text{at} \quad T = 0, \tag{3.3}$$

where $\hat{\pi}_1 = 0.05$ (case 1) or 0.01 (case 2). Results for case 1 are presented in figure 2. Grid-effect studies suggest that the accuracy achieved (with about 250 modes) is quite satisfactory. The most noticeable feature of the computational results as time T increases is the pronounced growth of $|P|$, accompanied by spanwise focusing and an accentuated minimum in Q. This feature leads on to the analysis below.

4. Finite-time blow-up

Given that the computational results of the previous section tend to suggest that a singularity may arise in the solution of the VWI system (3.1a, b) at finite time, we tried a number of possible analytical descriptions of a finite-time blow-up, say as $T \to T_s -$. The one that appears to be consistent is as follows.

In polar form, $P = R\exp(\mathrm{i}\theta)$ with R, θ real, and with $\rho \equiv R^2$, (3.1a, b) are replaced by the three real equations

$$\frac{1}{2}\frac{\partial \rho}{\partial T} + \frac{\partial}{\partial Z}\left(\rho \frac{\partial \theta}{\partial Z}\right) = \rho, \tag{4.1a}$$

$$\rho^2 \frac{\partial \theta}{\partial T} - \tfrac{1}{2}\rho \frac{\partial^2 \rho}{\partial Z^2} + \frac{1}{4}\left(\frac{\partial \rho}{\partial Z}\right)^2 + \rho^2\left(\frac{\partial \theta}{\partial Z}\right)^2 = -\rho^2 Q, \tag{4.1b}$$

$$\frac{\partial^2 Q}{\partial T^2} = \frac{\partial^2 \rho}{\partial Z^2} \tag{4.1c}$$

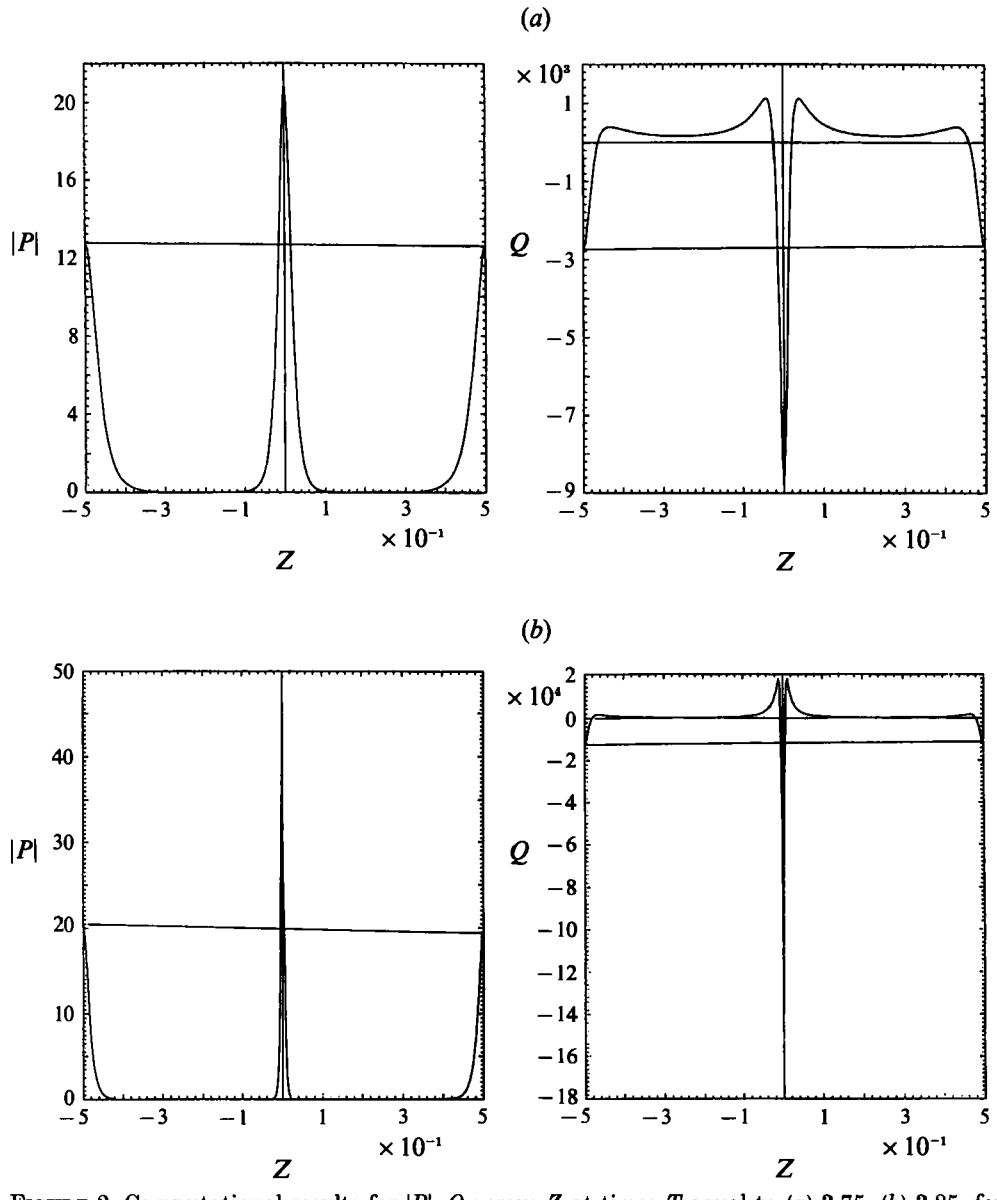

FIGURE 2. Computational results for $|P|$, Q versus Z at times T equal to (*a*) 3.75, (*b*) 3.85, for (3.1*a*, *b*) subject to (3.3).

for $(\rho, \theta, Q)(Z, T)$, and of course there is the integral property

$$\int_{-\infty}^{\infty} \rho(Z,T)\,\mathrm{d}Z = \mathrm{e}^{2T} \int_{-\infty}^{\infty} \rho(Z,0)\,\mathrm{d}Z \tag{4.1d}$$

from (4.1*a*). Then, as $T \to T_s-$, the proposed blow-up response has

$$\rho \sim (T_s - T)^{-2}\tilde{\rho}(\eta), \quad \theta \sim \tilde{\lambda}^2 K (T_s - T)^{-3} + \tilde{\theta}(\eta), \tag{4.2 a, b}$$

$$Q \sim \tilde{\lambda}^2 (T_s - T)^{-4}\tilde{Q}(\eta), \quad \text{with} \quad \eta \equiv \tilde{\lambda}(Z - Z_s)(T_s - T)^{-2}, \tag{4.2c, d}$$

near the singular location $Z = Z_s$. The constants $\tilde{\lambda}, K$ are unknown, and the orders in (4.2*a–d*) are implied by an order-of-magnitude argument applied to (4.1*a–d*).

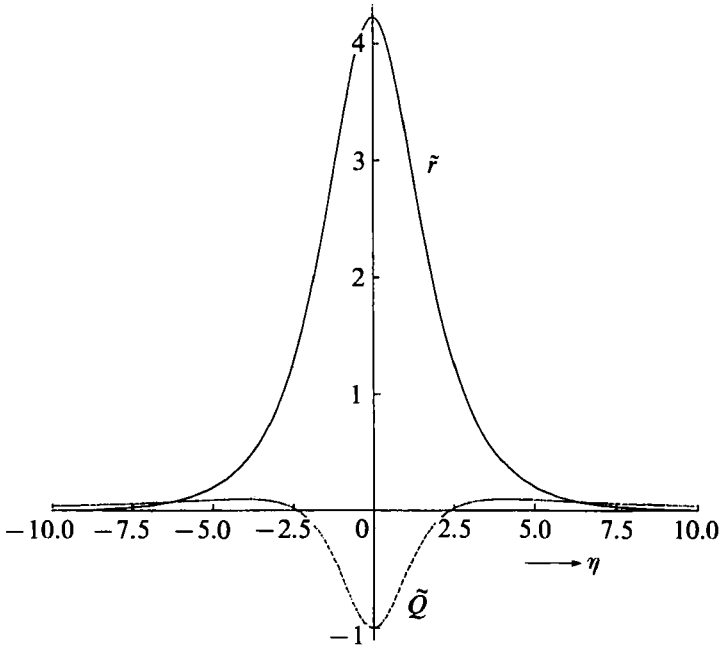

FIGURE 3. Numerical solution of the terminal form (4.3*c*), (4.4).

Substitution of (4.2*a–d*) into (4.1*a–c*) yields the nonlinear ordinary differential equations

$$(\tilde{\rho}\tilde{\theta}')' = 0, \quad 3K\tilde{\rho}^2 - \tfrac{1}{2}\tilde{\rho}\tilde{\rho}'' + \tfrac{1}{4}\tilde{\rho}'^2 + \tilde{\rho}^2\tilde{\theta}'^2 = -\tilde{\rho}^2\tilde{Q}, \tag{4.3a, b}$$

$$2\eta^2\tilde{Q}'' + 11\eta\tilde{Q}' + 10\tilde{Q} = \tfrac{1}{2}\tilde{\rho}'' \tag{4.3c}$$

at leading order, with a prime denoting $\mathrm{d}/\mathrm{d}\eta$. Here (4.3*a*) integrates to give $\tilde{\rho}\tilde{\theta}' = L$, an unknown constant, and so we are left with solving

$$3K\tilde{\rho}^2 - \tfrac{1}{2}\tilde{\rho}\tilde{\rho}'' + \tfrac{1}{4}\tilde{\rho}'^2 + L^2 = -\tilde{\rho}^2\tilde{Q}, \tag{4.3d}$$

coupled with (4.3*c*), for $\tilde{\rho}$, $\tilde{Q}$. In addition there is the condition

$$\int_{-\infty}^{\infty} \tilde{\rho}(\eta)\,\mathrm{d}\eta = O(1) \tag{4.3e}$$

to be satisfied, in view of the integral property (4.1*d*).

The large-η behaviour seems to require that $L = 0$, however, and so (4.3*d*) becomes

$$\tilde{r}'' = (\tilde{Q} + 3K)\tilde{r}, \quad \text{with} \quad \tilde{\rho} = \tilde{r}^2, \tag{4.4}$$

which, with (4.3*c*), govern $\tilde{r}$, $\tilde{\rho}$, $\tilde{Q}$. Here, at large η, in general $\tilde{r}$, $\tilde{\rho}$ decay exponentially and $\tilde{Q} \propto \eta^{-2}$ provided that K, which serves as an eigenvalue, is positive. The constant $\tilde{\lambda}$ in (4.2*b–d*) remains arbitrary, we note, being determined presumably by the initial conditions. So without loss of generality $\tilde{Q}(0)$ may be taken as ± 1 or zero, although the computational results of §3 suggest the value -1. Again, we assume here that $\tilde{r}$, $\tilde{\rho}$, $\tilde{Q}$ are even in η. A numerical solution of (4.3*c*), (4.4) with $\tilde{r}'(0) = \tilde{Q}'(0) = 0$, $\tilde{Q}(0) = -1$, $\tilde{r}(\pm\infty) = \tilde{Q}(\pm\infty) = 0$, indicates the value $K \approx 0.147$ and is presented in figure 3.

The analytical description in (4.2*a*)–(4.4) appears to agree with the computational results of §3, locally near blow-up, as the comparison in figure 4 shows. It is interesting that the blow-ups for cases 1, 2 seem to occur at $|Z| = 0$, 0.5 respectively.

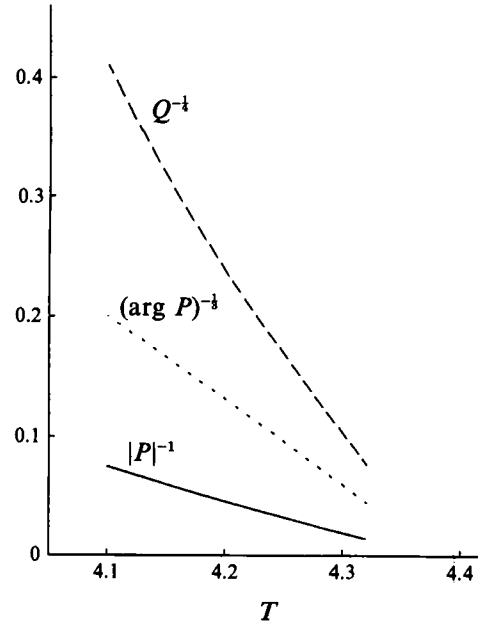

FIGURE 4. Comparisons between the computational results of §3 (shown in the figure) and the theory of §4; the latter predicts straight-line limiting behaviour as time T tends to T_s.

5. Further comments, repercussions, and comparisons with experiments

5.1. *Further comments and repercussions*

There are several points to make first about the flow structure discussed in §2. As elsewhere, e.g. Hall & Smith (1988, 1989, 1990, 1991), Bennett, Hall & Smith (1991), Smith & Walton (1989), Smith & Blennerhassett (1992), Smith (1992), the behaviour of the mean-flow correction or vortex part is most interesting. It is driven by wave-amplitude-squared forcing as in other configurations studied but acting here mainly in the bulk of the motion rather than being concentrated in a viscous wall layer or critical layer. The wave-amplitude forcing is relatively small but this is still sufficient to affect the spanwise-momentum balance of the slowly evolving vortex motion and hence, through continuity, the streamwise velocity of the vortex. Simultaneously the induced vortex flow acts to help control the development of the wave amplitude, thus provoking the interaction. The second harmonics, in contrast, play an insignificant role as they do not undergo a similar enhancing effect. Again, it is observed that the vortex contribution itself can produce a critical layer (at $\hat{y} = -b$ if this is positive, see also §3) which is additional to the main one, at $\hat{y} = 1$, but is believed to have negligible active influence on the whole interaction. Our current interest in any case is mostly in the purely temporal evolution where $|b| \to \infty$ in effect, as mentioned later. The effects of viscosity are also mentioned later.

Turning now to points that are more specific to the study in §§3, 4, we begin by noting that the VWI system (3.1*a*, *b*) exhibits strong secondary instability if the initial input is two-dimensional or nearly so. This aspect covers one of the issues raised in the introduction and is dealt with in Appendix B in some detail. The primary result is that the secondary instability increases with increasing input amplitude and/or with increasing spanwise variation ($\partial/\partial Z$). Similar results hold for other VWI's and related nonlinear interactions. Such instability acts merely as a precursor, of course, to the fully three-dimensional nonlinear case of (3.1*a*, *b*), which

then leads on to the nonlinear blow-up response of §4. It should be emphasized here that this is one of a number of paths through transition, in our opinion. An alternative is that which stays purely two-dimensional longer, avoiding secondary instability above and entering a nonlinear planar stage, as addressed and compared with experiments by Kachanov *et al.*(1992). The subsequent spike formation may be different for different paths; see also §5.2 and Smith & Bowles (1992). We should emphasize also that the present VWI holds for non-zero slow-time dependence and indeed our main interest here is in the purely temporal case where $\partial/\partial X_2 \equiv 0$. The purely spatial case, where $\partial/\partial T_2 \equiv 0$, is not covered, since then the constant b becomes zero, the buffer layer near the wall changes in character, and a different flow structure must hold. This is the subject of further study. The present VWI, then, is believed to yield the finite-time blow-up described in §4, for most reasonable initial and boundary conditions. The blow-up is local in space and so can apply even for non-periodic boundary conditions in Z. The viscous effect, i.e. the term P in the right-hand side of (3.1a), plays only a subsidiary role in the blow-up (see (4.1a), (4.3b)), despite playing a primary one elsewhere, e.g. in the earlier secondary instability of Appendix B and in Smith & Stewart (1987). Hence the actual blow-up behaviour is predominantly inviscid; see also the main repercussion addressed below in §5.2. Further, as far as we know, the present nonlinear case is the first, in the high-frequency range and related ones, to yield a blow-up within a finite time or distance.

A number of subsequent issues arise. For example, what happens if the effective frequency Ω is raised to $O(Re^{\frac{1}{4}})$, cf. Smith & Burggraf (1985) and below? What are the implications for VWI's with oblique-wave input, rather than near-planar, in this range? What then is their connection, if any, with the resonant triads of Craik (1971, 1985), Smith & Stewart (1987) which, it is interesting to observe, start with amplitudes similar to those in (2.3a, b) but do not exhibit blow-up as here? What are the analogues for compressible boundary layers and for channel flows (for the latter there would seem to be much similarity with the formations of streets in Nishioka *et al.*'s (1979) experiments, a matter now being investigated theoretically (Smith & Bowles 1992))? Further research is in progress on some of those issues.

5.2. *The main repercussion*

The major repercussion directly from the analysis and computations in §§2–4, however, concerns the flow response following the blow-up of §4. The orders of magnitude involved suggest that the next distinct stage (near $Z = Z_s$ at time $T \approx T_s$) arises when the wave amplitude $|p|$ increases to the order of $\Omega^{\frac{1}{2}}$, but with the typical streamwise velocities of the vortex then increasing to the order of $\Omega^{\frac{1}{2}}$ (because of (4.2c)), comparable with those of the basic flow, from (2.5a). This occurs when the timescale $(t-T_s)$ becomes as small as $O(\Omega^{-\frac{1}{4}})$, from (4.2a) with (2.2a), and the spanwise lengthscale $|Z-Z_s|$ is then decreased to $O(\Omega^{-\frac{1}{2}})$, from (4.2d) with (2.2c), a scale which is comparable with the shortest x-scale. Simultaneously, the typical vortex displacement $\propto A_{0M}$ is raised by a factor Ω whereas the typical wave displacement $\propto A_0$ is raised only by a factor $\Omega^{\frac{1}{4}}$, in view of (2.10c), thus introducing a relative effect of order $\Omega^{-\frac{3}{4}}$. The same relative effect is caused by the mean pressure which starts as $O(\Omega^{-\frac{3}{4}})$ in (2.3a), and in Appendix A, but then is found to rise to $O(\Omega^{-\frac{1}{2}})$ due to the growth of $|A_{0M}|$ mentioned above. Similar estimates may be made, e.g. for the spanwise velocity, which now increases to $O(\Omega^{-\frac{1}{4}})$ because of (4.2a, d) with (3.2), (2.10e), (2.5c). Hence this new stage has the form

$$u = \Omega^{\frac{1}{4}}\hat{U}_{0M} + \Omega^{-\frac{1}{4}}\hat{U}_1 + \ldots, \quad v = \Omega^{\frac{3}{4}}\hat{V}_0 + \hat{V}_1 + \ldots, \quad w = \Omega^{-\frac{1}{4}}\hat{W}_0 + \Omega^{-1}\hat{W}_1 + \ldots \tag{5.1a–c}$$

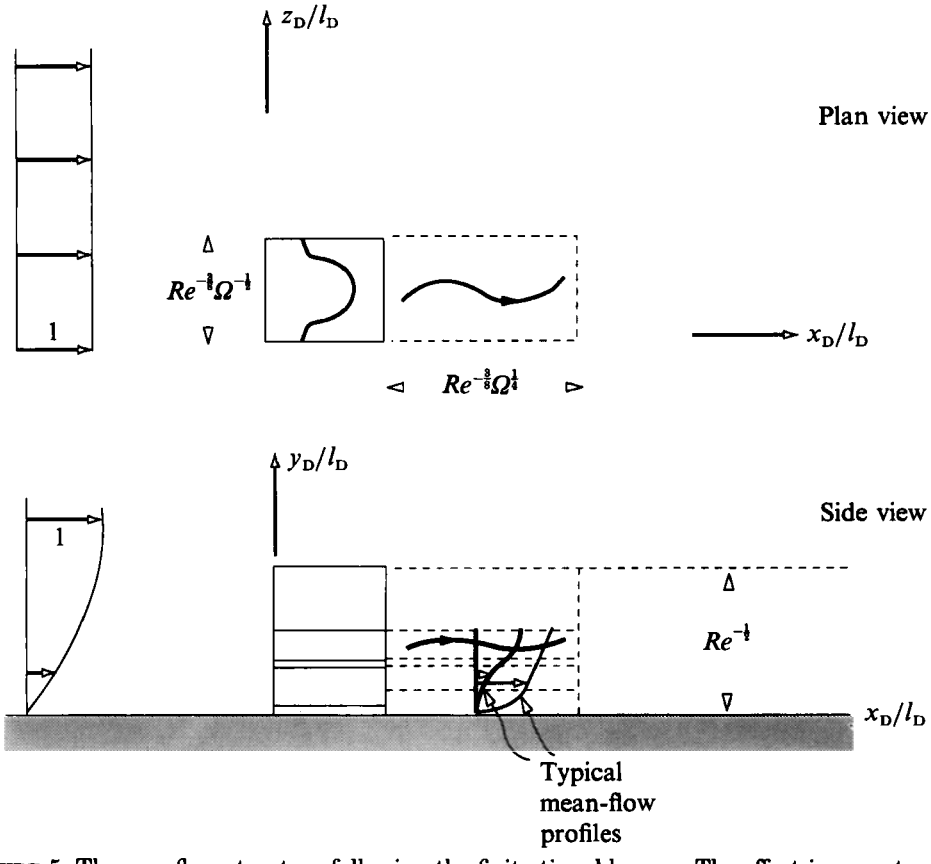

FIGURE 5. The new flow structure following the finite-time blow-up. The effect is now strongly nonlinear and more focused spanwise, as described in §5. Cf. figure 1.

for the velocities in the bulk of the flow where $\hat{y}$ is $O(1)$, with the unknown pressure and negative displacement given by

$$p = \Omega^{\frac{1}{2}}\hat{P}_0 + \Omega^{-\frac{1}{2}}\hat{P}_1 + \ldots, \quad A = \Omega^{\frac{1}{2}}\hat{A}_{0M} + \Omega^{-\frac{1}{2}}\hat{A}_1 + \ldots, \tag{5.1 d, e}$$

and the multi-scaling has

$$\frac{\partial}{\partial t} \to \frac{\Omega\partial}{\partial T_0} + \Omega^{\frac{1}{2}}\frac{\partial}{\partial \hat{T}} + \ldots, \quad \frac{\partial}{\partial X} \to \Omega^{\frac{1}{2}}\frac{\partial}{\partial X_0} + \Omega^{-\frac{1}{2}}\frac{\partial}{\partial \hat{X}} + \ldots, \quad \frac{\partial}{\partial Z} \to \Omega^{\frac{1}{2}}\frac{\partial}{\partial Z_0} + \ldots. \tag{5.2a–c}$$

The relative error generally is of order $\Omega^{-\frac{1}{2}}$ now. Here $\hat{U}_{0M}$, $\hat{A}_{0M}$ are slowly varying, i.e. independent of X_0, T_0, so that $\hat{U}_{0M}$ in particular gives the *total* mean-flow streamwise velocity in this regime. See also figure 5. Substituting into (2.1*a–c*) therefore yields, for the mean-flow terms first, the nonlinear governing equations

$$\frac{\partial \hat{U}_{0M}}{\partial \hat{X}} + \frac{\partial \hat{V}_{0M}}{\partial \hat{y}} + \frac{\partial \hat{W}_{0M}}{\partial Z_0} = 0, \tag{5.3a}$$

$$\frac{\partial \hat{U}_{0M}}{\partial \hat{T}} + \hat{U}_{0M}\frac{\partial \hat{U}_{0M}}{\partial \hat{X}} + \hat{V}_{0M}\frac{\partial \hat{U}_{0M}}{\partial \hat{y}} + \hat{W}_{0M}\frac{\partial \hat{U}_{0M}}{\partial Z_0} = 0, \tag{5.3b}$$

$$\frac{\partial \hat{W}_{0M}}{\partial \hat{T}} + \hat{U}_{0M}\frac{\partial \hat{W}_{0M}}{\partial \hat{X}} + \hat{V}_{0M}\frac{\partial \hat{W}_{0M}}{\partial \hat{y}} + \hat{W}_{0M}\frac{\partial \hat{W}_{0M}}{\partial Z_0} + F = -\frac{\partial \hat{P}_{1M}}{\partial Z_0}, \tag{5.3c}$$

where the subscript M denotes the mean-flow (vortex) component and the forcing term present is

$$F(\hat{X},\hat{y},Z_0,\hat{T}) = -\mathrm{i}\alpha_0\hat{U}_{11}\hat{W}_{01}^*+\mathrm{i}\alpha_0\hat{U}_{11}^*\hat{W}_{01}+\hat{V}_{01}\frac{\partial\hat{W}_{01}^*}{\partial\hat{y}}+\hat{V}_{01}^*\frac{\partial\hat{W}_{01}}{\partial\hat{y}}+\frac{\partial(\hat{W}_{01}\hat{W}_{01}^*)}{\partial Z_0}. \quad (5.3d)$$

Here 01, 11 denote the E-(wave) components, where

$$E \equiv \exp[\mathrm{i}(\alpha_0 X_0 - T_0)], \quad (5.4)$$

with α_0 a real function of $\hat{X}$, $\hat{T}$ but unknown (strictly $\alpha_0 X_0$ should be replaced by $\Omega^{\frac{1}{2}}\int\alpha_0\,\mathrm{d}\hat{X}$), and the wave terms are controlled by

$$\mathrm{i}\alpha_0\hat{U}_{11}+\partial\hat{V}_{01}/\partial\hat{y}+\partial\hat{W}_{01}/\partial Z_0 = 0, \quad (5.5a)$$

$$-\mathrm{i}\hat{U}_{11}+\mathrm{i}\alpha_0\hat{U}_{0\mathrm{M}}\hat{U}_{11}+\hat{V}_{01}\partial\hat{U}_{0\mathrm{M}}/\partial\hat{y}+\hat{W}_{01}\partial\hat{U}_{0\mathrm{M}}/\partial Z_0 = -\mathrm{i}\alpha_0\hat{P}_{01}, \quad (5.5b)$$

$$-\mathrm{i}\hat{W}_{01}+\mathrm{i}\alpha_0\hat{U}_{0\mathrm{M}}\hat{W}_{01} = -\partial\hat{P}_{01}/\partial Z_0, \quad (5.5c)$$

again from (2.1a–c). The boundary conditions for the vortex and wave systems above include the tangential-flow and displacement constraints

$$\hat{V}_{0\mathrm{M}} = 0, \quad \hat{V}_{01} = 0 \quad \text{at} \quad \hat{y} = 0, \quad (5.6a)$$

$$\hat{U}_{0\mathrm{M}} \sim \hat{y}+\hat{A}_{0\mathrm{M}}, \quad \hat{W}_{0\mathrm{M}}\to 0, \quad \hat{U}_{11}\to\hat{A}_{11}, \quad \hat{W}_{01}\to 0 \quad \text{as} \quad \hat{y}\to\infty, \quad (5.6b)$$

from (2.1d–e) (see also below and Appendix C), combined with the pressure–displacement laws

$$\frac{\partial\hat{P}_{1\mathrm{M}}}{\partial Z_0} = \frac{1}{\pi}\frac{\partial^2}{\partial\hat{X}^2}\int_{-\infty}^{\infty}\hat{A}_{0\mathrm{M}}(\hat{X},s)\frac{\mathrm{d}s}{Z_0-s} \quad (5.6c)$$

$$\left.\begin{aligned}(-\alpha_0^2+\partial^2/\partial Y^2+\partial^2/\partial Z_0^2)\bar{P}_{01} = 0, \quad \bar{P}_{01}\ \text{bounded},\\ \bar{P}_{01}\to\hat{P}_{01},\ \partial\bar{P}_{01}/\partial Y\to -\alpha_0^2\hat{A}_{11} \quad \text{as} \quad Y\to 0,\end{aligned}\right\} \quad (5.6d)$$

linking $\hat{P}_{1\mathrm{M}}$ with $\hat{A}_{0\mathrm{M}}$ and $\hat{P}_{01}$ with $\hat{A}_{11}$ respectively, due to (2.1f–h). In (5.6c) the single-integral form stems from the fact that the x-variation is slow for the mean terms, while in (5.6d) Y equals $\bar{y}\Omega^{\frac{1}{2}}$. Although $\hat{U}_{0\mathrm{M}}$, which appears among the coefficients in (5.5a–c), is unknown it is a slow function in the streamwise direction and this allows some further simplification. Thus solving (5.5a–c) for $\hat{U}_{11}$, $\hat{V}_{01}$, $\hat{W}_{01}$ as in Smith (1979c) and applying (5.6a, b) we obtain

$$\hat{W}_{01} = \mathrm{i}(\alpha_0\hat{U}_{0\mathrm{M}}-1)^{-1}\partial\hat{P}_{01}/\partial Z_0, \quad (5.7a)$$

$$\hat{V}_{01} = -\mathrm{i}(\alpha_0\hat{U}_{0\mathrm{M}}-1)\int_0^{\hat{y}}\left\{\frac{\partial^2\hat{P}_{01}/\partial Z_0^2-\alpha_0^2\hat{P}_{01}}{(\alpha_0\hat{U}_{0\mathrm{M}}-1)^2}-2\alpha_0\frac{(\partial\hat{U}_{0\mathrm{M}}/\partial Z_0)(\partial\hat{P}_{01}/\partial Z_0)}{(\alpha_0\hat{U}_{0\mathrm{M}}-1)^3}\right\}\mathrm{d}\hat{y}, \quad (5.7b)$$

with $\hat{U}_{11}$ then following from (5.5a), and

$$\alpha_0^2\hat{A}_{11} = \left\{\frac{\partial^2\hat{P}_{01}}{\partial Z_0^2}-\alpha_0^2\hat{P}_{01}+\frac{\partial\hat{P}_{01}}{\partial Z_0}\frac{\partial}{\partial Z_0}\right\}I, \quad (5.8a)$$

where

$$I \equiv \int_0^{\infty}(\hat{U}_{0\mathrm{M}}-\alpha_0^{-1})^{-2}\,\mathrm{d}\hat{y}. \quad (5.8b)$$

Further, the results (5.7a, b) enable F in (5.3d) to be reduced to the form

$$F(\hat{X},\hat{y},Z_0,\tilde{T}) = \frac{1}{(\hat{U}_{0\mathrm{M}}-\alpha_0^{-1})^2}\frac{\partial}{\partial Z_0}\left[|\hat{P}_{01}|^2+\frac{1}{\alpha_0^2}\left|\frac{\partial\hat{P}_{01}}{\partial Z_0}\right|^2\right], \quad (5.9)$$

after some manipulation.

So we are left now with a VWI in which the vortex part $[\hat{U}_{0M}, \hat{V}_{0M}, \hat{W}_{0M}, \hat{A}_{0M}, \hat{P}_{1M}]$ has to satisfy (5.3*a–c*), subject to the boundary conditions in (5.6*a–c*) and the wave-forcing F in (5.9), and the wave part $[\hat{P}_{01}, \hat{A}_{11}]$ is governed by (5.8*a*, *b*) coupled with (5.6*d*).

The principal features of this new VWI so far are the following.

(*a*) It is strongly nonlinear, since in particular the total mean flow is now affected locally (see 5.1*a*)), and the vortex and the wave parts must be solved together because of the coupling via F in (5.9) and via the integral I in (5.8*a*, *b*). This strong nonlinearity arises while the wave amplitudes are still small.

(*b*) The wave-forcing F here is again active essentially throughout the local flow field. Certain new effects are present now, compared with those described in §2, including more inertial terms in (5.3 *b*, *c*) and the spanwise pressure gradient in (5.3*c*), the $\hat{W}_{01}\hat{W}_{01}^{*}$ inertial effect in (5.3*d*) and the $|\partial\hat{P}_{01}/\partial Z_0|^2$ contribution in (5.9), as well as the strong nonlinearity, although the mean streamwise pressure gradient still has negligible influence (see (5.3*b*)). Further, the spanwise dependence continues to be non-simple.

(*c*) The proposed VWI flow structure above is unusual in that it is predominantly inviscid, as could be anticipated from §4. On the other hand, viscous effects are expected to re-enter the reckoning through a different mechanism in due course. For, as (5.6*a*) indicates, the three-dimensional viscous sublayers nearer the wall are assumed to be passive and attached; yet they are unlikely to remain so in many cases. See also Appendix C. This connects with the non-interactive singularity of Van Dommelen (1981), Elliott, Cowley & Smith (1983), and with the studies of interactive break-up, sublayer eruption and vortex formation in Smith (1988), Peridier *et al.* (1991*a*, *b*), Hoyle, Smith & Walker (1991, 1992), Hoyle (1992), Smith & Bowles (1922) (who show quite close agreement with experiments on the first spike) and with continuing theoretical work.

(*d*) There is also the question of whether the critical layer occurring near the position where $\hat{U}_{0M} = \alpha_0^{-1}$ (see (5.7*a*)–(5.9)) can remain passive as in the original flow structure of §2. The critical layer is again nonlinear but now it is fully three-dimensional, its position being dependent on $\hat{X}, Z_0, \hat{T}$ since $\hat{U}_{0M}$ is no longer a small perturbation of $\hat{y}$ in general. Along with this, there is the possibility that vortex/Rayleigh-wave interactions may be provoked in addition if the profile $\hat{U}_{0M}$ becomes sufficiently inflexional (see also (*e*) below), and again new critical-layer effects are very active then (Hall &Smith 1991), although that is at the inflexion point.

(*e*) Nonlinear finite-time break-up in the new VWI system is a strong possibility, in the manner described by Smith (1988) and extended to three dimensions by Hoyle *et al.* (1991), Hoyle (1992). The integral I in (5.8*b*) forms a link with the 1988 paper.

(*f*) Obviously there are many other intriguing, and difficult, issues to be addressed. Possible limiting solutions of the new VWI could be helpful. The regime where $\Omega \to O(Re^{\frac{1}{4}})$ could be of interest, where the flow structure moves into Euler scales, with the dominant streamwise length shrinking to $O(Re^{-\frac{1}{4}})$ as in Smith & Burggraf (1985) but with the vortex streamwise lengthscale elongating to $O(Re^{-\frac{5}{16}})$, and likewise for the timescales, in view of (5.2*b*). Many of the previous comments apply equally well to that regime.

It seems clear then that a powerful new effect is produced, as summarized by (5.3*a–c*), (5.6*a–d*), (5.8*a*, *b*), (5.9). Hence the VWI studied in the present §§2–4 provides a means for relatively small near-planar input disturbances (as in (2.3*a*, *b*),

(2.4), (2.5a–c)) to gain '$O(1)$' (strong nonlinear) status sooner, because of three-dimensional interaction leading to the blow-up in §4, rather than later as would be the case in purely two-dimensional evolution (Smith & Burggraf 1985).

The nonlinear blow-up and the associated spanwise focusing here seem to agree with the findings of Klebanoff & Tidstrom (1959) and subsequent experiments; further, the agreement is enhanced by the interactive-break-up predictions summarized in (c) above, as a comparison with the experimental oscillogram of characteristic breakdowns shown in Stuart's (1963) figure IX.26 indicates. Experimental comparisons are given below.

5.3. *Comparisons with experiments*

Here we make a number of comparisons between the present theory and the original experiments of Klebanoff & Tidstrom (1959) as given in Stuart (1963). These experiments show nonlinear effects leading on to turbulence between the lower and upper branches, typically, and so we can examine the applicability of the current theory.

Of interest first are the graphical results presented in Stuart's (1963) figures IX.26–28. In figure IX.26, a comparison of the typical spanwise z-scale of 1 in. with the typical mean-flow streamwise evolution scale (X_2) of 3 in. suggests taking the value $\Omega = 9$, in view of (2.2b, c).

The theory then implies that the z-scale associated with spanwise focusing into streets and strong nonlinearity is reduced by a factor $\Omega^{-\frac{1}{4}}$ (from (5.2c)), thus predicting the new z-scale to be $\frac{1}{3}$ in. See the comparisons in figure 6(a), which seem favourable.

The theory also predicts that the perturbation velocity u' of the wave part increases by a factor $\Omega^{\frac{1}{4}}$ (see (5.1a), (2.5a)), i.e. by $\sqrt{3}$, while the vortex velocity increases by a factor Ω, i.e. by 9. Again the comparisons in figure 6(a) seem favourable.

Concerning frequency dependence, Stuart (1963, p. 575) records that reducing the input frequency by a factor of approximately 2 increases the typical u'/U_1 (where U_1 is the local free-stream velocity) by a factor of about 2 experimentally. In comparison, the theory implies an amplitude $\propto \Omega^{-\frac{1}{4}}$ (from (2.5a)), i.e. a factor $\sqrt{2}$.

Also, later in the transition process, 'breaking into turbulence' occurs experimentally (Stuart, p. 575) at a value of u'/U_1 of about 0.074. This compares favourably with the bulk value of u'/U_1 predicted theoretically in §5.2 as $Re^{-\frac{1}{4}}\Omega^{-\frac{1}{4}}$ from (5.1a), or 0.071, based on the ratio of the typical y-scale (0.046 in.) to the initial z-scale (1 in.), which varies as $Re^{-\frac{1}{4}}\Omega^{\frac{1}{4}}$ from (1.1c) with (2.2c)ff.

Further, the above bulk value varies only relatively slowly (like $\Omega^{-\frac{1}{4}}$) with the frequency Ω, in line with Stuart's comment in line 8 of his page 575.

The velocity values in Stuart's figure IX.27 are also not inconsistent with the scalings of (2.5a), for the experimental values for the original basic-flow, vortex and wave parts are about 0.3, 0.03, 0.02, i.e. in ratio 10:1:0.7, whereas the theoretical ratio is Ω:1:1, i.e. 9:1:1. See figure 6(b).

The trend in Stuart's figure IX.28 concerning the influence of increasing the input amplitude, which promotes the breakdown, likewise seems in keeping with the theory. Thus increasing the input amplitude P by a factor μ_1, say, in (3,1a, b), is accommodated simply by factors μ_1^{-1}, $\mu_1^{-\frac{1}{2}}$, μ_1 in T (or T_2, X_2), Z_1, Q in turn, with the linear growth term in (3.1a) assumed negligible. So the theory predicts that the product of the input amplitude and the x-evolution length up to blow-up remains approximately constant. This product, for the three experimental runs leading to

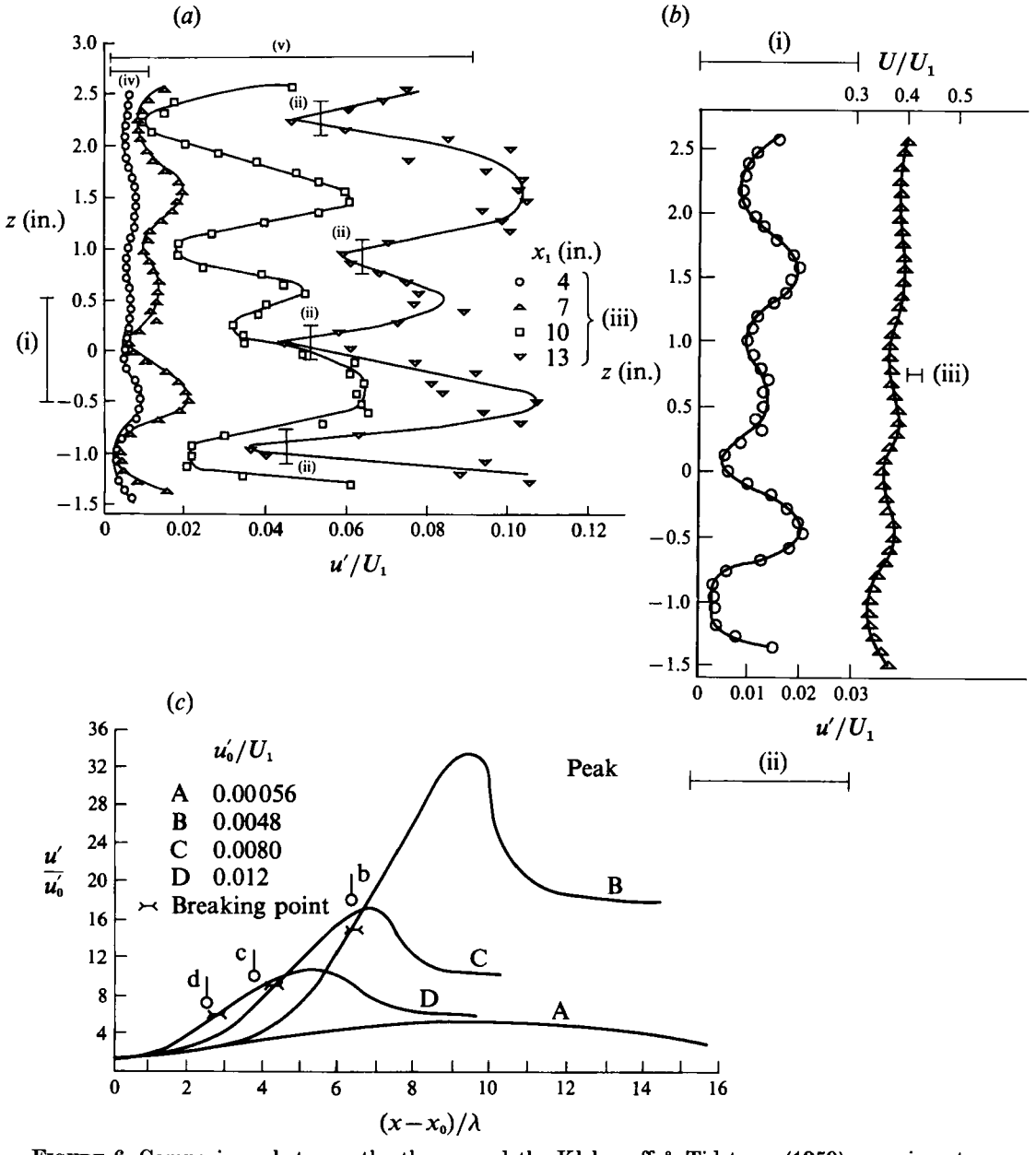

FIGURE 6. Comparisons between the theory and the Klebanoff & Tidstrom (1959) experiments; (*a–c*) are taken respectively from Stuart's (1963) figs. IX. 26–28; see §5.3. (*a*) Comparing theoretical spanwise lengthscales (i), (ii) (vertical bars), streamwise lengthscale (iii), and velocity scales (iv), (v) (horizontal bars), with the experimental measurements of non-dimensional velocities versus z at various streamwise locations x_1. (This z and that in (*b*) below are different from the coordinate introduced earlier in the text). (*b*) Comparing theoretical velocity scales (i)–(iii) (horizontal bars) with the experimental measurements of u'/U_1 (○) and U/U_1 (△) versus z, where U denotes the mean velocity, and $x_1 = 7$ in. (*c*) Comparing theoretical blow-up locations (marked b, c, d, according to the relation (input amplitude) × (distance) equals constant, as described in §5.3) with the breaking-point locations found experimentally as shown, for the respective cases B, C, D. Here b is lined-up for case B, with c, d then evaluated as above; notation here is as in Stuart (1963).

blow-up in the above figure, has the values 0.0048×6.3, 0.0080×4.3, 0.012×2.8, i.e. 0.0302, 0.0344, 0.0336, which, indeed, are not far from constant. See also figure 6(*c*).

Some of the nine or so comparisons listed above are summarized in figure 6(*a–c*). The overall agreement seems good in order-of-magnitude terms at least. Moreover, in response to a comment by Professor S. N. Brown, we observe that the z-station at which the blow-up of §4 takes place is a peak rather than a valley, if a peak is characterized (as in Stuart 1963) by energy enhancement. More significant perhaps is the fact that a scale change is produced in the variation of the mean boundary-layer displacement which mostly *increases* rapidly in the blow-up (since the variation is effectively $-A_{0M}$ which is proportional to $-Q$, see also figure 4). Simultaneously, the wall shear stress, being proportional to $-Q$ here, also mostly increases rapidly however, due to a combination of critical layer and three-dimensional effects.

There may be other explanations of course, e.g. VWI's nearer the lower branch as in Smith & Walton (1989, see especially their §5 where spanwise focusing is again possible) or nearer the upper branch, but the evidence so far tends to suggest that the current theory captures much of the heart of the experimental findings for this type of boundary-layer transition.

The referees' helpful comments are gratefully acknowledged; and thanks are due to SERC for support of P.A.S. during 1987–89 and for computing facilities and to AFOSR (grant no. 89–0475) and the United Technologies Independent Research Program for support of F.T.S.

Appendix A. The external pressure–displacement relations

To obtain the successive components in the pressure–displacement interaction, we prefer to address (2.1*g*, *h*) rather than (2.1*f*). Guided by (2.3*a*), the outer pressure $\bar{p}$ expands as

$$\bar{p} = \bar{P}_0 + \Omega^{-1}\bar{P}_2 + O(\Omega^{-m}), \tag{A 1}$$

where the x,z-dependence is as in (2.2*b*, *c*), $\bar{y} = \Omega^{-\frac{1}{2}}Y$ mostly, and the power m is found below. From (2.1*g*), the governing equations for $\bar{P}_0$, $\bar{P}_2$ are

$$\left(\frac{\partial^2}{\partial X_0^2} + \frac{\partial^2}{\partial Y^2}\right)\bar{P}_0 = 0, \tag{A 2}$$

$$\left(\frac{\partial^2}{\partial X_0^2} + \frac{\partial^2}{\partial Y^2}\right)\bar{P}_2 = -2\frac{\partial^2 \bar{P}_0}{\partial X_0 \partial X_2} - \frac{\partial^2 \bar{P}_0}{\partial Z_1^2}. \tag{A 3}$$

Hence the solutions are given by

$$\bar{P}_0 = \bar{P}_{01}E + \text{c.c.}, \quad \bar{P}_2 = \bar{P}_{21}E + \ldots + \text{c.c.}, \tag{A 4}$$

with $\bar{P}_{01} = P_0 \mathrm{e}^{-Y}$, $\bar{P}_{21} = (P_{21} + \pi_{21}Y)\mathrm{e}^{-Y}$, where $\pi_{21} = \mathrm{i}\dfrac{\partial P_0}{\partial X_2} + \dfrac{1}{2}\dfrac{\partial^2 P_0}{\partial Z_1^2}$. (A 5)–(A 7)

Here the matching condition on $\partial\bar{p}/\partial\bar{y}$ in (2.1*h*) confirms the results $P_0 = A_0, \alpha_0 = 1$ in (2.10*c*, *d*), at leading order, followed by the relation

$$-P_{21} + \pi_{21} = 2\mathrm{i}\,(\partial A_0/\partial X_2) - A_{21}, \tag{A 8}$$

from (A 6). Then use of (A 8) with (A 7), (2.10*c*) leads to the law quoted in (2.15*c*).

Other successive terms in the expansion may be determined similarly, although there is some subtlety about the mean-flow (vortex) contributions, of which the main one is driven by the term $\Omega^{-\frac{1}{4}}A_{0M}E^0$ in (2.3*b*). This has no fast dependence on x and so forces only a contribution $O(\Omega^{-\frac{3}{4}})$ to $\partial^2 A/\partial x^2$ in (2.1*h*), given (2.2*b*). Further, the $\bar{y}$-scale for the mean-flow terms stays as $O(1)$, to balance the z-scale in effect. So the third-order term in (A 1) must include

$$\Omega^{-\frac{3}{4}}\bar{P}_M(X_2, \bar{y}, Z_1, T_2)E^0 \quad (m = \tfrac{3}{2}). \tag{A 9}$$

Substitution into (2.1*g*, *h*) then yields the quasi-two-dimensional cross-plane problem

$$\left(\frac{\partial^2}{\partial \bar{y}^2}+\frac{\partial^2}{\partial Z_1^2}\right)\bar{P}_M = 0, \quad \text{with} \quad \frac{\partial \bar{P}_M}{\partial \bar{y}} \to \frac{\partial^2 A_{0M}}{\partial X_2^2} \quad \text{as} \quad \bar{y} \to 0, \tag{A 10}$$

and with far-field boundedness as usual. Hence the induced surface pressure has

$$\bar{P}_M \text{ [at } \bar{y} = 0+] = \frac{1}{\pi}\int_{-\infty}^{\infty} \frac{\partial \hat{A}}{\partial \xi}(X_2, \xi, T_2)\frac{d\xi}{Z_1 - \xi} \tag{A 11}$$

where

$$\partial^2 \hat{A}/\partial Z_1^2 \equiv \partial^2 A_{0M}/\partial X_2^2, \tag{A 12}$$

and as anticipated in (2.3*a*) the mean-flow-correction pressure at the surface is only $O(\Omega^{-\frac{3}{4}})$, specifically $\Omega^{-\frac{3}{4}}$ times (A 11).

Appendix B. On secondary instability of purely two-dimensional flow

For the pure two-dimensional case the Z-derivatives and Q in (3.1*a*, *b*) vanish identically, so that the exact solution has

$$P = \tilde{b}\,e^T, \quad Q = 0, \tag{B 1}$$

with $\tilde{b}$ being a complex constant. To examine the secondary instability of this solution (cf. Bayly, Orszag & Herbert 1988; Smith & Stewart 1987) we consider a small perturbation of (B1), in the form

$$(\rho, \theta, Q) = (\tilde{B}\,e^{2T}, 0, 0) + \tilde{\epsilon}(\tilde{\rho}, \tilde{\theta}, \tilde{Q}) + O(\tilde{\epsilon}^2) \tag{B 2}$$

with $\tilde{\epsilon}$ small and $\tilde{B} = |\tilde{b}|^2$ since $\rho = |P|^2$. Substitution into (3.1*a*, *b*) or equivalently (4.1*a*–*c*) then yields the linear equations

$$\frac{1}{2}\frac{\partial \tilde{\rho}}{\partial T}+\tilde{B}e^{2T}\frac{\partial^2 \tilde{\theta}}{\partial Z^2} = \tilde{\rho}, \quad \tilde{B}e^{2T}\frac{\partial \tilde{\theta}}{\partial T}-\frac{1}{2}\frac{\partial^2 \tilde{\rho}}{\partial Z^2} = -\tilde{B}e^{2T}\tilde{Q}, \quad \frac{\partial^2 \tilde{Q}}{\partial T^2} = \frac{\partial^2 \tilde{\rho}}{\partial Z^2}, \tag{B 3–B 5}$$

for the perturbations. From (B 3)–(B 5) and taking spanwise periodicity such that $(\tilde{\rho}, \tilde{\theta}, \tilde{Q}) = (\tilde{\tilde{\rho}}, \tilde{\tilde{\theta}}, \tilde{\tilde{Q}})\cos(\beta Z)$ we therefore obtain the ordinary differential equation

$$\tilde{\tilde{Q}}^{iv} - 4\tilde{\tilde{Q}}''' + (4+\beta^4)\tilde{\tilde{Q}}'' - 2\beta^4 \tilde{B}e^{2T}\tilde{\tilde{Q}} = 0 \tag{B 6}$$

for $\tilde{\tilde{Q}}(T)$.

So if there is no initial two-dimensional wave then $\tilde{B} = 0$ and the vortex effect $\tilde{\tilde{Q}}$ grows as $\exp(2T \pm i\beta^2 T)$ at most. By contrast, the presence of the two-dimensional wave, i.e. $\tilde{B} \neq 0$, provokes the vortex growth

$$\tilde{\tilde{Q}} \propto \exp[2^{\frac{1}{4}}\beta \tilde{B}^{\frac{1}{4}}\exp(T/2)] \tag{B 7}$$

at large times T. Thus, as in a number of other interactions studied, pronounced three-dimensional secondary instability to vortex motion is produced, of the exp(exp) form.

Appendix C. On the flow nearer the surface, in the strongly nonlinear stage

This Appendix concerns the small-$\hat{y}$ properties of the strongly nonlinear VWI stage of §5.2 and the two resultant viscous layers – a nonlinear buffer zone and a quasi-linear Stokes zone – nearer the surface. The buffer in particular introduces significant new features as anticipated in item (*c*) in §5.2.

First, (5.3*b*) indicates that the total mean velocity $\hat{U}_{0M}$ is conserved along all the particle paths, after starting out as identically equal to $\hat{y}$. Hence $\hat{U}_{0M}$ remains zero at $\hat{y} = 0+$. Generally, for small $\hat{y}$,

$$[\hat{U}_{0M}, \hat{V}_{0M}, \hat{W}_{0M}] \sim [\lambda_1 \hat{y}, \mu_1 \hat{y}, \nu_0 + \nu_1 \hat{y}] + \ldots, \tag{C 1}$$

where the unknown coefficients satisfy, from (5.3*a–c*),

$$\mu_1 + \frac{\partial \nu_0}{\partial Z_0} = 0, \quad \frac{\partial \lambda_1}{\partial \hat{T}} + \mu_1 \lambda_1 + \nu_0 \frac{\partial \lambda_1}{\partial Z_0} = 0, \quad \frac{\partial \nu_0}{\partial \hat{T}} + \nu_0 \frac{\partial \nu_0}{\partial Z_0} + F_0 = -\frac{\partial \hat{P}_{1M}}{\partial Z_0}, \tag{C 2)–(C 4}$$

and F_0 denotes the value of (5.9) at $\hat{y} = 0+$.

Second, there is therefore a viscous buffer zone for the total mean-flow components, given by $y = \Omega^{-\frac{1}{8}} y_1$ with y_1 of $O(1)$ and the underlying expansions

$$u = \Omega^{-\frac{1}{8}} U^{(0)} + \Omega^{-\frac{1}{4}} U^{(1)} + \ldots, \tag{C 5}$$

$$v = \Omega^{\frac{1}{8}} V^{(0)} + O(\Omega^{-\frac{1}{4}}) + \Omega^{-\frac{1}{2}} V^{(1)} + \Omega^{-\frac{5}{8}} V^{(2)} + \ldots \tag{C 6}$$

$$w = \Omega^{-\frac{1}{4}} W^{(0)} + \Omega^{-\frac{3}{8}} W^{(1)} + \Omega^{-1} W^{(2)} + \ldots \tag{C 7}$$

for the velocities; see also (C 24) later. The pressure and displacement remain as in (5.1*d*, *e*), while (5.2*a–c*) describe the multi-scaling present, with $U^{(0)}$ being independent of X_0, T_0. Substitution into (2.1*a–c*) then yields the successive governing equations, from the continuity and the streamwise and spanwise momentum balances respectively,

$$\frac{\partial U^{(1)}}{\partial X_0} + \frac{\partial V^{(0)}}{\partial y_1} + \frac{\partial W^{(0)}}{\partial Z_0} = 0, \quad \frac{\partial U^{(0)}}{\partial \hat{X}} + \frac{\partial V^{(1)}}{\partial y_1} + \frac{\partial W^{(1)}}{\partial Z_0} = 0 \tag{C 8), (C 9}$$

$$\frac{\partial U^{(1)}}{\partial T_0} = -\frac{\partial \hat{P}_0}{\partial X_0}, \quad \frac{\partial U^{(0)}}{\partial \hat{T}} + \frac{\partial U^{(6)}}{\partial T_0} + U^{(0)} \frac{\partial U^{(1)}}{\partial X_0} + V^{(0)} \frac{\partial U^{(0)}}{\partial y_1} + W^{(0)} \frac{\partial U^{(0)}}{\partial Z_0} = \frac{\partial^2 U^{(0)}}{\partial y_1^2}, \tag{C 10), (C 11}$$

$$\frac{\partial W^{(0)}}{\partial T_0} = -\frac{\partial \hat{P}_0}{\partial Z_0}, \tag{C 12}$$

$$\frac{\partial W^{(2)}}{\partial T_0} + \frac{\partial W^{(0)}}{\partial \hat{T}} + U^{(1)} \frac{\partial W^{(0)}}{\partial X_0} + V_0 \frac{\partial W^{(0)}}{\partial y_1} + W^{(0)} \frac{\partial W^{(0)}}{\partial Z_0} = -\frac{\partial \hat{P}_1}{\partial Z_0} + \frac{\partial^2 W^{(0)}}{\partial y_1^2}; \tag{C 13}$$

the new feature here is the appearance of the viscous terms in the right-hand sides of (C 11), (C 13), as expected. Hence (C 8), (C 10), (C 12) show that the main *wave part* is given by the simple expressions

$$U^{(11)} = \alpha_0 \hat{P}_{01}, \quad W^{(01)} = -\mathrm{i} \frac{\partial \hat{P}_{01}}{\partial Z_0}, \quad V^{(01)} = -\mathrm{i} \left\{ \alpha_0^2 \hat{P}_{01} - \frac{\partial^2 \hat{P}_{01}}{\partial Z_0^2} \right\} y_1 \tag{C 15), (C 16}$$

for the E-components, which match with the bulk solution via (5.7*a*, *b*). The *total mean-flow or vortex part* in contrast is controlled by the viscous nonlinear system

$$\frac{\partial V^{(0M)}}{\partial y_1} + \frac{\partial W^{(0M)}}{\partial Z_0} = 0, \quad \frac{\partial U^{(0)}}{\partial \hat{T}} + V^{(0M)} \frac{\partial U^{(0)}}{\partial y_1} + W^{(0M)} \frac{\partial U^{(0)}}{\partial Z_0} = \frac{\partial^2 U^{(0)}}{\partial y_1^2}, \tag{C 17), (C 18}$$

$$\frac{\partial W^{(0M)}}{\partial \hat{T}} + V^{(0M)}\frac{\partial W^{(0M)}}{\partial y_1} + W^{(0M)}\frac{\partial W^{(0M)}}{\partial Z_0} + F^{(0)} = -\frac{\partial \hat{P}_{1M}}{\partial Z_0} + \frac{\partial^2 W^{(0M)}}{\partial y_1^2}, \tag{C 19}$$

from (C 8), (C 11), (C 13), where $F^{(0)}$ comes from the mean-flow part of the three nonlinear terms in (C 13) and can be shown to be equal to F_0 (in (C 4)), using (C 14)–(C 16), so that

$$F^{(0)} = \frac{\partial}{\partial Z_0}\left\{\alpha_0^2|\hat{P}_{01}|^2 + \left|\frac{\partial \hat{P}_{01}}{\partial Z_0}\right|^2\right\}. \tag{C 20}$$

Thus the buffer's mean-flow responds as a quasi-two-dimensional unsteady boundary layer *in the cross-plane*, for $V^{(0M)}$, $W^{(0M)}$ in (C 17), (C 19), with the wave-amplitude-squared forcing $F^{(0)}$ effectively acting here as an extra contribution to the spanwise pressure gradient, and with the $\hat{X}$-variation remaining secondary. The boundary conditions are

$$W^{(0M)} \to \nu_0 \quad (\text{with} \quad V^{(0M)} \sim \mu_1 y_1) \quad \text{as} \quad y_1 \to \infty, \tag{C 21}$$

$$W^{(0M)} = V^{(0M)} = 0 \quad \text{at} \quad y_1 = 0. \tag{C 22}$$

Here $\nu_0(\hat{X}, Z_0, \hat{T})$ is to be determined from the outer inviscid bulk solution, as in §5.2 and (C 2), (C 4). Hence as ν_0 varies, the system (C 17), (C 19)–(C 22) is able to follow a path towards the Van Dommelen (1981) non-interactive singularity in a finite time; after that the interactive finite-time singularity of Smith (1988) and other features of recent and continuing study as mentioned in (*c*) of §5.2 can come into force. This development competes with the possible development of a singularity in the bulk motion of §5.2 (see (*e*) there).

Afterwards in effect (C 18) serves to fix the streamwise mean velocity $U^{(0)}$, subject to $U^{(0)}$ asymptoting to $\lambda_1 y_1$ as $y_1 \to \infty$ and being zero at $y_1 = 0$. Thus the scaled mean streamwise wall shear will be altered still further, as it takes the values 1 at large $\hat{y}$ in the bulk, λ_1 at small $\hat{y}$ or large y_1, and $\partial U^{(0)}/\partial y_1$ at small y_1 in the buffer.

Third, there is a Stokes layer, a zone closer to the wall and performing the usual task of reducing the wave velocities to zero at the surface. This viscous zone has $y = \Omega^{-\frac{1}{8}}\tilde{y}$ with $\tilde{y}$ of order unity and

$$u = \Omega^{-\frac{1}{4}}u_w + \ldots + O(\Omega^{-\frac{1}{2}}\,\text{vortex}), \tag{C 23}$$

$$v = \Omega^{-\frac{1}{4}}v_w + \ldots + O(\Omega^{-\frac{5}{8}}\,\text{vortex}), \tag{C 24}$$

$$w = \Omega^{-\frac{1}{4}}w_w + \ldots + O(\Omega^{-\frac{5}{8}}\,\text{vortex}). \tag{C 25}$$

The governing equations here are quasi-linear, however, so that the leading terms in (C 23)–(C 25) have the usual Stokes form. The $\tilde{y}$-dependent term that is found in the asymptote of v_w in (C 24) at large $\tilde{y}$ gives a viscous displacement effect (cf. §2), and this is responsible for the $O(\Omega^{-\frac{1}{4}})$ contribution, which is independent of y_1, in (C 6).

The buffer-zone system in (C 17)–(C 22) confirms the re-emerging importance of viscosity in a new nonlinear way in the transition process, during the strongly nonlinear stage, despite the suppression of linear viscous effects earlier (see §§4, 5). It is interesting also that the singularities referred to above for the buffer-flow system (C 17)–(C 22) are predominantly for the spanwise flow, in contrast to the bulk flow of §5.2.

REFERENCES

Bassom, A. P. & Hall, P. 1990 *Stud. Appl. Maths.*

Bayly, B. J., Orszag, S. A. & Herbert, T. 1988 *Ann. Rev. Fluid Mech.* **20**, 359–391.

Bennett, J., Hall, P. & Smith, F. T. 1991 *J. Fluid Mech.* **223**, 475–495.

Borodulin, V. I. & Kachanov, Y. S. 1988 *Proc. Siberian Div. USSR Acad. Sci., Tech. Sci.* **18**, 65–77 (in Russian). (See also *Sov. J. Appl. Phys.* **3** (2), 70–81, 1989, in English.)

CRAIK, A. D. D. 1971 *J. Fluid Mech.* **50**, 393–413.

CRAIK, A. D. D. 1985 In *Proc. IUTAM Symp. on Laminar–Turbulent Transition*, 1984, *Novosibirsk, USSR* (ed. W. Kozlov). Springer.

ELLIOTT, J. W., COWLEY, S. J. & SMITH, F. T. 1983 *Geophys. Astrophys. Fluid Dyn.* **25**, 77–138.

HALL, P. & SMITH, F. T. 1988 *Proc. R. Soc. Lond.* A **417**, 255–282.

HALL, P. & SMITH, F. T. 1989 *Eur. J. Mech.* B **8**, 179–205.

HALL, P. & SMITH, F. T. 1990 In *Instability and Transition*, Vol. II (ed. M. Y. Hussaini & R. G. Voigt), pp. 5–39 Springer.

HALL, P. & SMITH, F. T. 1991 *J. Fluid Mech.* **227**, 641–666.

HAMA, F. R. & NUTANT, J. 1963 *Proc. Heat Transer Fluid Mech. Inst.* 77–93.

HOYLE, J. M. 1992 Extensions to the theory of finite-time breakdown in unsteady interactive boundary layers. Ph.D. thesis, University of London.

HOYLE, J. M., SMITH, F. T. & WALKER, J. D. A. 1991 *Comput. Phys. Commun.* **65**, 151.

HOYLE, J. M., SMITH, F. T. & WALKER, J. D. A. 1992 On sublayer eruption and vortex formation; part 2. (in preparation).

KACHANOV, Y. S. 1988 Experimental results on stability of separating flow.

KACHANOV, Y. S. & LEVCHENKO, V. Y. 1984 *J. Fluid Mech.* **138**, 209.

KACHANOV, Y. S., RYZHOV, O. S. & SMITH, F. T. 1992 Formation of solitons in transitional boundary layers: theory and experiments. *J. Fluid Mech.* (submitted).

KLEBANOFF, P. S. & TIDSTROM, K. D. 1959 *NASA TN* D-195.

KLEBANOFF, P. S., TIDSTROM, K. D. & SARGENT, L. M. 1962 *J. Fluid Mech.* **12**, 1–34.

KLEISER, L. & ZANG, T. A. 1991 *Ann. Rev. Fluid Mech.* **23**, 495–437.

KOVASZNAY, L. S. G., KOMODA, H. & VASUDEVA, B. R. 1962 *Proc. Heat Transfer & Fluid Mech. Inst.* 1–26.

NISHIOKA, M., ASAI, M. & IIDA, S. 1979 In *Laminar-Turbulent Transition. IUTAM Mtg, Stuttgart.*

PERIDIER, V. J., SMITH, F. T. & WALKER, J. D. A. 1991*a* *J. Fluid Mech.* **232**, 99–131.

PERIDIER, V. J., SMITH, F. T. & WALKER, J. D. A. 1991*b* *J. Fluid Mech.* **232**, 133–165.

SCHUBAUER, G. B. & SKRAMSTAD, H. K. 1947 *Rep. Natl Adv. Comm. Aero., Wash.* 909.

SMITH, F. T. 1979*a* *Proc. R. Soc. Lond.* A **366**, 91–109.

SMITH, F. T. 1979*b* *Proc. R. Soc. Lond.* A **368**, 573–589.

SMITH, F. T. 1979*c* *Mathematika* **26**, 187–223.

SMITH, F. T. 1985 *Utd. Tech. Res. Cent. Rep.* 85–36.

SMITH, F. T. 1986*a* *J. Fluid Mech.* **169**, 353–377.

SMITH, F. T. 1986*b* *Utd. Tech. Res. Cent. Rept.* 86–10.

SMITH, F. T. 1988 *Mathematika* **35**, 256–273.

SMITH, F. T. 1992 *Phil. Trans. R. Soc. Lond.* A (in press).

SMITH, F. T. & BLENNERHASSETT, P. 1992 *Proc. R. Soc. Lond.* A **436**, 585–602.

SMITH, F. T. & BOWLES, R. I. 1992 Transition theory and experimental comparisons on (*a*) amplification into streets and (*b*) a strongly nonlinear break-up criterion. *Proc. R. Soc. Lond.* A (submitted).

SMITH, F. T. & BURGGRAF, O. R. 1985 *Proc. R. Soc. Lond.* A **399**, 25–55.

SMITH, F. T., DOORLY, D. J. & ROTHMAYER, A. P. 1990 *Proc. R. Soc. Lond.* A **428**, 255–281.

SMITH, F. T. & STEWART, P. A. 1987 *J. Fluid Mech.* **179**, 227.

SMITH, F. T. & WALTON, A. G. 1989 *Mathematika* **36**, 262–289.

STEWART, P. A. & SMITH, F. T. 1987 *Proc. R. Soc. Lond.* A **409**, 229–248.

STUART, J. T. 1963 *Laminar Boundary Layers* (ed. L. Rosenhead), Ch. IX. Oxford University Press.

VAN DOMMELEN, L. 1981 Unsteady boundary-layer separation. Ph.D. thesis, Cornell University.

WALTON, A. G. & SMITH, F. T. 1992 *J. Fluid Mech.* **244**, 649–676.

ZHUK, V. I. & RYZHOV, O. S. 1982 *Dok. Akad. Nauk. SSSR* **263** (1), 56–69 (in Russian).